

12-2013

Microwave-assisted synthesized SAPO-56 as a catalyst in the conversion of CO₂ to cyclic carbonates.

Zhenzhen Xie 1988-
University of Louisville

Follow this and additional works at: <http://ir.library.louisville.edu/etd>

Recommended Citation

Xie, Zhenzhen 1988-, "Microwave-assisted synthesized SAPO-56 as a catalyst in the conversion of CO₂ to cyclic carbonates." (2013). *Electronic Theses and Dissertations*. Paper 1602.
<https://doi.org/10.18297/etd/1602>

This Master's Thesis is brought to you for free and open access by ThinkIR: The University of Louisville's Institutional Repository. It has been accepted for inclusion in Electronic Theses and Dissertations by an authorized administrator of ThinkIR: The University of Louisville's Institutional Repository. This title appears here courtesy of the author, who has retained all other copyrights. For more information, please contact thinkir@louisville.edu.

MICROWAVE-ASSISTED SYNTHESIZED SAPO-56 AS A CATALYST IN THE
CONVERSION OF CO₂ TO CYCLIC CARBONATES

By

Zhenzhen Xie

B.S. Material Chemistry, Heilongjiang University, July 2011

A Thesis

Submitted to the Faculty of the
University of Louisville
J. B. Speed School of Engineering
in Partial Fulfillment of the Requirements
for the Professional Degree

MASTER OF SCIENCE

Department of Chemical Engineering
University of Louisville
Louisville, Kentucky

December 2013

MICROWAVE-ASSISTED SYNTHESIZED SAPO-56 AS A CATALYST IN THE
CONVERSION OF CO₂ TO CYCLIC CARBONATES

Zhenzhen Xie

A Thesis Approved On

08/15/2013

(Date)

by the Following Reading and Examination Committee:

Dr. Moises Carreon, Thesis Director

Dr. Xiaohan Fu

Dr. Eric Berson

Dr. Gamini Sumanesekera

ACKNOWLEDGEMENTS

First of all, I would like to express my deepest appreciation to my advisor, Dr Moises A. Carreon, who gave me the golden opportunity throughout my work. It would not have been possible without his professional advice and guidance. More importantly, I really appreciate his kindness and understanding in the last two years.

Special thanks to Dr. Sean Fu, Dr. Eric Berson and Dr. Gamini Sumanesekera, thesis committee members, for their suggestions to complete my thesis.

I also would like to thank Minqi, Apolo and Masoudeh for their assistance in the lab. They always have discussions with me whenever I confronted any difficulties. I also would like to thank all the staff and technicians in Department of Chemical Engineering, University of Louisville, who helped me in solving all the problems, and I came to know about so many new things. Thanks also to all my friends who have helped me in finishing my MS degree.

My greatest thankfulness goes to my family for their love and support and kind co-operation and encouragement, which help me in completion of my thesis.

ABSTRACT

MICROWAVE-ASSISTED SYNTHESIZED SAPO-56 AS A CATALYST IN THE
CONVERSION OF CO₂ TO CYCLIC CARBONATES

Zhenzhen Xie

08/15/2013

The effective utilization of CO₂ as a renewable raw material for the production of useful chemicals is an area of great interest. In particular, the catalytic conversion of CO₂ into cyclic carbonates, which are useful chemical intermediates employed for the production of plastics and organic solvents, represents an attractive route for the efficient use of carbon dioxide. Microporous crystals, including zeolites and metal organic frameworks (MOFs), and mesoporous ordered oxides possess many desirable properties, which make them appealing for cycloaddition reactions. In general, these porous materials display chemical and thermal stability, moderate to high CO₂ uptakes, an open porous structure for improved mass transfer, accessible pore volumes, acid sites which are known as active sites for cycloaddition reactions, high surface areas.

SAPOs (silicoaluminophosphates), a particular type of small pore molecular sieves, have received considerable interest because of their applications in separations, catalysis, and adsorption. Their unique functional properties are associated with their chemical and thermal stability, unique shape selectivity, molecular sieving properties, ordered microporous crystalline structure, and surface properties. SAPO-56 is a

crystalline microporous silicoaluminophosphate in which silicon substitutes for some of the phosphorous and aluminum atoms in the structural framework. The AFX topology of SAPO-56 is characterized by a three dimensional structure with pore cages arranged in interconnected networks, with window (pore size) sizes of $\sim 3.4 \times 3.6$ Å. Due to its pore size similar to the kinetic diameter of several relevant gas molecules such as CO₂, CH₄, O₂, N₂ as well as due to relatively high CO₂ uptakes, SAPO-56 may find potential applications for CO₂ conversion to useful chemicals.

A conventional hydrothermal synthesis approach used to synthesize SAPO-56 requires typically long synthesis times (days) and relatively high hydrothermal temperatures (200 °C). Microwave heating offers several advantages over conventional heating, such as fast crystallization, phase selectivity, narrow particle size distribution, abundant nucleation, morphology and size control and rapid and uniform heating. Herein we present the synthesis of SAPO-56 crystals via microwave heating. The resultant crystals displayed high catalytic activity in the synthesis of chloropropene carbonate from CO₂ and epichlorohydrin. The Microwave as-synthesized SAPO-56 displayed crystal size as $\sim 3-4$ μm, while the crystal size hydrothermal as-synthesized SAPO-56 is ~ 50 μm. When $3-4$ μm crystals were used, the yield to chloropropene carbonate was 84.8%, whereas the yield to the carbonate was only 42.2% when crystals of about 50 μm were used. The enhanced catalytic activity of SAPO-56 crystals was related to their high CO₂ adsorption capacity, small crystal size, and the presence of acid sites. In addition, silica nanospheres present in the surface of the smaller SAPO-56 crystals may display a role as specific surface sites for the cycloaddition reaction. For this

particular reaction, SAPO-56 seems to be robust catalytic phase because it can be recycled without loss in the catalytic activity.

TABLE OF CONTENTS

ACKNOWLEDGEMENTS	III
ABSTRACT.....	IV
LIST OF TABLES	IX
LIST OF FIGURES	X
CHAPTER 1 INTRODUCTION	1
1.1 Environmental and energy concerns for carbon dioxide	1
1.2 Motivation of producing chemicals from CO ₂	3
1.3 Objectives of this work	3
CHAPTER 2 BACKGROUND	5
2.1 Introduction to Zeolites	5
2.2 SAPO-56.....	7
2.3 Zeolite synthesis method.....	8
2.3.1 Self-Assembly-Hydrothermal-Assisted Approach	8
2.3.2 Microwave heating approach.....	10
2.4 Catalytic synthesis of carbonates	12
CHAPTER 3 EXPERIMENTAL APPROACH	14
3.1 Synthesis of SAPO-56 crystals via hydrothermal synthesis	14
3.2 Synthesis SAPO-56 via microwave approach	15

3.3	Characterization	16
3.4	SAPO-56 catalyzed CO ₂ conversion to carbonates.....	18
3.5	Equipment	19
3.5.1.	Hydrothermal synthesis of SAPO-56.....	19
3.5.2.	Reaction	22
3.5.3.	SAPO-56 Characterization.....	23
CHAPTER 4 RESULTS AND DISCUSSION		26
4.1	Characterization of SAPO-56.....	26
4.2	Catalytic activity	32
CHAPTER 5 CONCLUSIONS		38
CHAPTER 6 FUTURE DIRECTIONS		39
REFERENCES		40
APPENDIX.....		43
CURRICULUM VITAE.....		45

LIST OF TABLES

Table 1 Selected properties and catalytic performance of SAPO-56 in the cycloaddition of CO ₂ to epichlorohydrin.....	34
--	----

LIST OF FIGURES

Figure 1 World energy consumption by fuel	2
Figure 2 Global CO ₂ emissions from fossil-fuels	2
Figure 3 SAPO-56 crystal structures	8
Figure 4 Schematic showing the catalytic conversion of CO ₂ into a cyclic carbonate.....	13
Figure 5 SAPO-56 crystals synthesis procedure using hydrothermal method	15
Figure 6 SAPO-56 crystal syntheses via MW	16
Figure 7 Hydrothermal Autoclave with 50mL Teflon Vessel ³⁶	19
Figure 8 Hydrothermal Synthesis oven.....	20
Figure 9 Eppendorf Centrifuge	21
Figure 10 Programming oven	21
Figure 11 Microwave instrument.....	22
Figure 12 Parr Reactor Model 4576A.....	23
Figure 13 Nova Nano SEM 600.....	23
Figure 14 X-Ray Diffraction.....	24
Figure 15 Micromeritics Tristar 3000 Porosimeter	24
Figure 16 Micromeritics Autochem 2910	25
Figure 17 NMR.....	25
Figure 18 (a) XRD pattern and (b) SEM image of SAPO-56 crystals synthesized via microwave heating at 150 °C and 250 psi for 10 minutes. *Denotes SAPO-17. (c) XRD pattern and (d) SEM image of SAPO-56 crystals synthesized via	

conventional hydrothermal treatment. The same gel composition was used for both samples.....	26
Figure 19 HRTEM of (a) hexagonal SAPO-56 crystals synthesized via microwave heating at 150 °C and 250 psi for 10 minutes, (b) silica nanospheres present at the surface of the SAPO-56 crystals, (c) higher magnification of the ~25 nm silica nanospheres, (d) rod-like crystals corresponding to SAPO-17.....	28
Figure 20 EDS distribution analysis for MW and hydrothermal synthesized samples. ...	29
Figure 21 ²⁹ Si NMR of (a) MW synthesized and (b) hydrothermally synthesized SAPO-56.....	30
Figure 22 SAED patterns (left) and radial intensity distribution profiles (right) of SAPO-56 crystals synthesized via microwave heating at 150 °C and 250 psi for 10 minutes. MC03 and MC06 refer to two different analyzed micro-crystals.	31
Figure 23 (a) XRD patterns of MW heated synthesized SAPO-56 crystals at 30 minutes and 120 minutes. Representative SEM images of the sample synthesized at (b) 30 minutes and (b) 120 minutes.	32
Figure 24 Yield to chloropropene carbonate at different temperature for hydrothermal synthesized SAPO-56.	33
Figure 25 CO ₂ uptakes for SAPO-56 crystals synthesized via (a) microwave assisted approach and (b) hydrothermal treatment.	35
Figure 26 Correlation between Yield to chloropropene carbonate (%) and CO ₂ uptake for different catalysts: (a) ZIF-8, (b) Cu-MOF, ⁴² (c) SAPO-56 (HT), (d) SAPO-56 (MW). Reaction conditions for all catalysts: 100 °C, 4 hr, 18 mmol of epichlorohydrin and 100 mg of catalyst. CO ₂ uptakes taken at 400 Torr.	36

Figure 27 NH₃-TPD of (a) MW synthesized and (b) hydrothermally synthesized SAPO-
56..... 37

CHAPTER 1 INTRODUCTION

1.1 Environmental and energy concerns for carbon dioxide

The concentration of greenhouse gases like CO₂, CH₄, NO_x in the environment are increasing at fast rate since the beginning of industrial revolution. In particular, carbon dioxide is the primary greenhouse gas emitted through human activities. In 2011, CO₂ accounted for about 84% of all U.S. greenhouse gas. CO₂ emissions have increased dramatically, mainly due to the combustion of fossil fuels, such as coal, natural gas and oil for the energy and transportation, although certain industrial processes and land-use changes also emit CO₂. The CO₂ emissions from different sources are shown in Figure 1.¹ Figure 2² shows that global carbon emissions from fossil fuels have significantly increased since 1900. Emissions increased by over 16 times between 1900 and 2008.

Carbon dioxide concentrations in the atmosphere have been increasing over the past century compared to the rather steady level evident during the pre-industrial era (about 280 parts per million in volumes, or ppmv) and is now linked to climate change.³ The 2005 concentration of CO₂ (379 ppmv) was about 35% higher than in the mid-1800s, with the fastest growth occurring in the past years (1.9 ppmv/year in the period 1995-2005). Significant increases have also occurred in levels of methane and nitrous oxide.

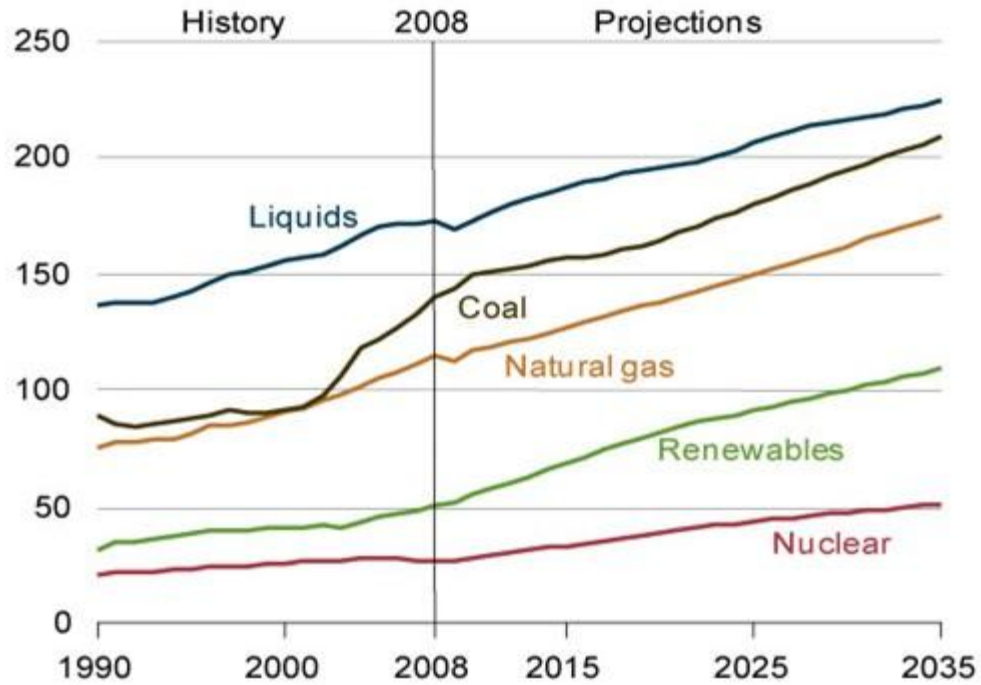


Figure 1 World energy consumption by fuel

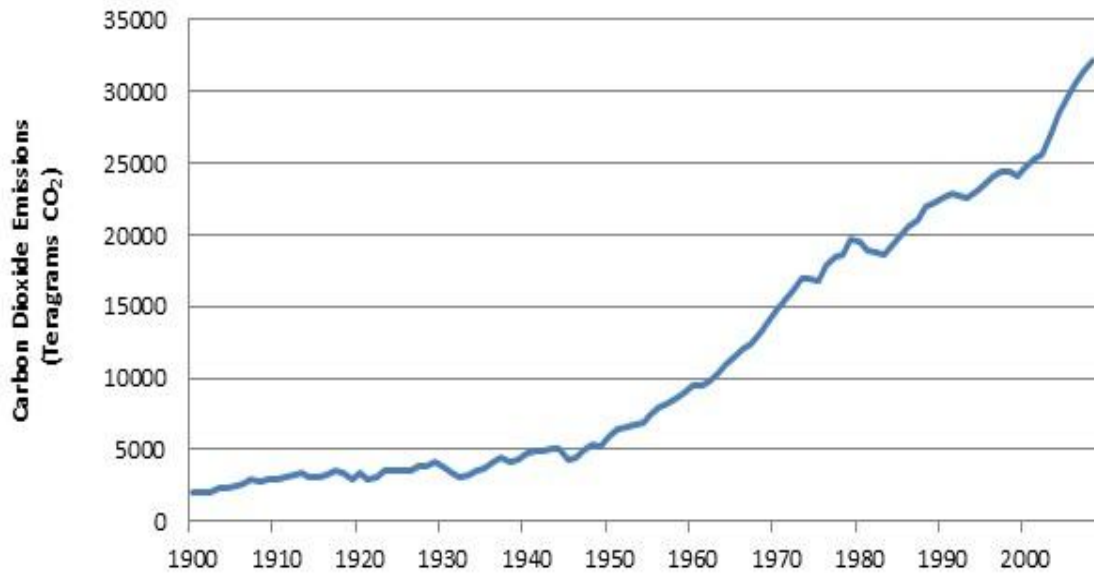


Figure 2 Global CO₂ emissions from fossil-fuels

As these gases, especially CO₂, continue to increase, potential adverse effects on regional and global climate, ecosystem function, and human health increase as well. The main solution being proposed to allow continued energy generation by combustion of

fossil fuels whilst stabilizing global atmospheric carbon dioxide levels is carbon capture and storage (CCS) in which the CO₂ is separated, purified, pressurized and transported for long term underground or undersea storage.⁴ However, CCS is a very energy intensive process which has been estimated to require around 30% of the total energy produced by a power station.

Instead of just dumping the CO₂, it is attractive to consider utilizing it in the large scale production of chemicals. In this way, an unwanted waste product can be turned into a valuable commodity.

1.2 Motivation of producing chemicals from CO₂

There is an increasing trend to consider carbon dioxide as a raw material resource and a business opportunity rather than a waste with a cost of disposal. Carbon dioxide is a cheap, non-toxic and non-flammable feedstock that can frequently replace toxic chemicals such as phosgene or isocyanates. CO₂ is a totally renewable feedstock compared to oil or coal. The production of chemicals from CO₂ can lead to totally new materials such as polymers. New routes to existing chemical intermediates and products could be more efficient and economical than current methods. The production of chemicals from CO₂ could have a small but significant positive impact on the global carbon balance.

1.3 Objectives of this work

The specific objectives are:

- 1) Synthesis of SAPO-56 crystals via microwave assisted thermal approach
- 2) Study the catalytic performance of SAPO-56 crystals in the conversion of CO₂ into cyclic carbonates.

- 3) Establish fundamental structure/catalytic relationships of SAPO-56 catalysts in the conversion of CO₂ into cyclic carbonates.

CHAPTER 2 BACKGROUND

Zeolites are one of the most important porous materials for wide variety of applications, including catalysts. In this chapter, generalities on zeolites are presented. Structural features and different synthesis methods employed for SAPO-56 are described. The importance and advantages of microwave heating as an alternative approach to prepare zeolite crystals is highlighted. In the second part of this chapter we present the mechanism of the CO₂ reaction to cyclic carbonates.

2.1 Introduction to Zeolites

Zeolites are crystalline minerals that are broadly present in nature and have been known to mankind for almost 250 years. Zeolite molecular sieves comprise a class of microporous, crystalline compounds composed of three-dimensional network of atoms such as Si, Al, P, etc. These tetrahedrally coordinated atoms (T atoms) are coordinated to four oxygen atoms and are linked to other T atoms by sharing each oxygen with a neighboring T-atom tetrahedron. Zeolites exhibit very uniform pore size distribution, high specific surface area, high porosity, variable chemical composition and controllable acid-base properties.

Today, synthetic zeolites are used commercially more often than natural zeolites due to the purity of crystalline products and the uniformity of particle sizes. The sources for early synthesized zeolites were standard chemical reagents. Much of the study of

basic zeolite science was done on natural zeolites. The main advantages of synthetic zeolites in comparison to naturally-occurring zeolites are that they can be engineered with a wide variety of chemical properties and pore sizes and that they have greater thermal stability. Zeolite synthesis involves the hydrothermal crystallization of aluminosilicate gels (formed upon mixing an aluminate and silicate solution in the presence of alkali hydroxides and/or organic bases), or solutions in a basic environment. The crystallization is in a closed hydrothermal system at increasing temperature, autogeneous pressure and varying time (few hours to several days). Nowadays, it is still very difficult to have a deep understanding of the formation mechanism and crystallization of zeolites because the type of zeolite is affected by the following factors ²⁹⁻³¹:

(1) Composition of the reaction mixture (silica to alumina ratio; OH^- ; inorganic cations). First, increasing the Si/Al ratio strongly affects physical properties of the zeolites. Second, OH^- modifies the nucleation time by influencing transport of silicates from the solid phase to solution. Third, inorganic cations act as structure directing agents and balance the framework charge. They affect the crystal purity and product yield.

(2) Nature of reactants and their pretreatments. The zeolite synthesis is carried out with inorganic as well as organic precursors. The inorganic precursors yielded more hydroxylated surfaces whereas the organic precursors easily incorporated the metals into the network.

(3) Temperature of the process. The rate of crystallization is directly proportional to temperature while the rate of nucleation is inversely proportional to temperature.

(4) Reaction time. Crystallization parameter must be adjusted to minimize the production of the other phases while also minimizing the time needed to obtain the desired crystalline phase.

(5) pH of the reaction mixture. The process of zeoliteization is carried out in alkaline medium ($\text{pH} > 10$).

(6) Other factors. The synthesis can be carried out on a continuous or semi continuous mode, which enhances the capacity, making it compatible for industrial applications.

Nowadays, zeolites are available on a large scale and in a variety of applications. Zeolites are mainly used as ion exchangers in laundry detergents where they remove calcium and magnesium from water by exchanging it for sodium present in the zeolite. Furthermore, zeolites are applied as adsorbents in the purification of gas streams to remove water and volatile organic species, and in the separation of different isomers and gas-mixtures, moreover they are applied in the clean-up of radioactive waste. However, here the focus will entirely be on the application of zeolites as catalysts.

2.2 SAPO-56

SAPOs (silicoaluminophosphates), a particular type of small pore molecular sieves, have received considerable interest because of their applications in separations,³² catalysis,³³ and adsorption.³⁴ Their unique functional properties are associated with their chemical and thermal stability, unique shape selectivity, molecular sieving properties, ordered microporous crystalline structure, and surface properties. SAPO-56 is a crystalline microporous silicoaluminophosphate in which silicon substitutes for some of

the phosphorous and aluminium atoms in the structural framework.³⁵ The AFX topology of SAPO-56 is characterized by a three dimensional structure with pore cages arranged in interconnected networks, with window (pore size) sizes of $\sim 3.4 \times 3.6 \text{ \AA}$.^{35c} The framework of AFX is shown in Figure 3. Due to its pore size similar to the kinetic diameter of several relevant gas molecules such as CO_2 , CH_4 , N_2 , O_2 as well as due to relatively high CO_2 uptakes,^{35d} SAPO-56 may find potential applications for CO_2 capture from natural gas or flue gas and /or CO_2 conversion to useful chemicals.

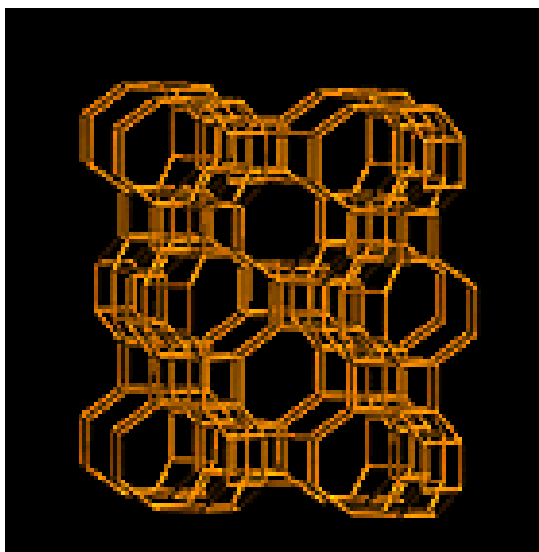


Figure 3 SAPO-56 crystal structures

2.3 Zeolite synthesis method

2.3.1 Self-Assembly-Hydrothermal-Assisted Approach

Hydrothermal synthesis is a method to produce different chemical compounds and materials using closed system physical and chemical processing flowing in aqueous solutions at temperatures above $100 \text{ }^\circ\text{C}$ and pressure above 1 atm. Hydrothermal research was initiated in the middle of the 19th century by geologists and was aimed at laboratory

simulations of natural hydrothermal phenomena. Later in the 20th century, hydrothermal synthesis was clearly identified as an important technology for material synthesis, predominantly in the fields of hydrometallurgy and single crystal growth.¹¹

Hydrothermal synthesis method is a process that utilizes single or heterogeneous phase reactions in aqueous media at elevated temperature ($T > 25\text{ }^{\circ}\text{C}$) and pressure ($P > 100\text{ kPa}$) to crystallize ceramic materials directly from solution. However, researchers also use this term to describe processes conducted at ambient conditions. Syntheses are normally conducted at autogeneous pressure, which corresponds to the saturated vapor pressure of the solution at the specified temperature and composition of the hydrothermal solution. Upper limits of hydrothermal synthesis extend to over $1000\text{ }^{\circ}\text{C}$ and 500 MPa pressures.¹² However, mild conditions are preferred for commercial processes where temperatures are less than $350\text{ }^{\circ}\text{C}$ and pressure less than 50 MPa . Intensive research has led to a better understanding of hydrothermal chemistry, which has significantly reduced the reaction time, temperature and pressure for hydrothermal crystallization of materials ($T < 200\text{ }^{\circ}\text{C}$, $P < 1.5\text{ MPa}$).^{13, 14, 15} This breakthrough has made hydrothermal synthesis more economical since processes can be engineered using cost-effective and proven pressure reactor technology and methodologies already established by the chemical process industry.

Hydrothermal synthesis offers many advantages over conventional and non-conventional synthetic methods. The ability to precipitate already crystallized powders directly from solution regulates the rate and uniformity of nucleation, growth and aging, which results in improved control of size and morphology of crystallites and significantly reduced aggregation levels, which is not possible with many other synthesis processes.¹⁶

The purity of hydrothermally synthesized powders significantly exceeds the purity of the starting materials. Hydrothermal processing can take place in a wide variety of combinations of aqueous and solvent mixture-based systems. In general, processing with liquids allows for automation of a wide range of unit operations such as charging, transportation, mixing and product separation. Moreover, relative to solid state processes, liquids give a possibility for acceleration of diffusion, adsorption, reaction rate and crystallization, especially under hydrothermal conditions.¹⁴ However, unlike many advanced methods that can prepare a large variety of forms and chemical compounds, such as chemical vapor-based methods, the respective costs for instrumentation, energy and precursors are far less for hydrothermal methods. Hydrothermal methods are more environmentally benign than many other synthesis methods, which can be attributed in part to energy conserving low processing temperatures, absence of milling, ability to recycle waste, and safe and convenient disposal of waste that cannot be recycled.¹⁴ The low reaction temperatures also avoid other problems encountered with high temperature processes, for example poor stoichiometry control due to volatilization of components (e.g., Pb volatilization in Pb-based ceramics).

2.3.2 Microwave heating approach

The reduction of zeolite crystal size has been a major research field for the past several years as the decrease of dimension leads to substantial changes in the properties of the materials.¹⁷ This has an impact on the performance of zeolites in applications such as catalysis and separation.^{18, 19} Additionally, this development has led to developments of new synthesis strategies yielding nanosize materials with narrow particle size distributions.

Conventional heating has a heat source on the outside and relies on transferring the heat to the surface of the material and then conducting the heat to the middle of the material. Compared with conventional heating, microwave dielectric heating has the following advantages for chemical synthesis ²⁰ (thermal effects of microwave):

- a) the introduction of microwave energy into a chemical reaction can lead to much higher heating rates than those which are achieved conventionally;
- b) the microwave energy is introduced into the chemical reactor remotely without direct contact between the energy source and the reacting chemicals;
- c) it is volumetric and instantaneous (or rapid) heating with no wall or heat diffusion effects;
- d) it can realize selective heating because chemicals and the containment materials for chemical reactions do not interact equally with microwaves;
- e) “hot spots” yielded on local boundaries by reflections and refractions may result in a “super-heating” effect, which can be described best as local overheating and is comparable to the delayed boiling of overheated liquids under conventional conditions.

The first patent on MW synthesis was reported on the synthesis of zeolite A. ²¹ Since then, MW heating has been widely used in the synthesis of different zeolite compositions ^{22, 23} including catalysts, ²⁴ membranes, ²⁵ and films. ²⁶ Comprehensive reviews on zeolite synthesis using MW have been reported. ^{27, 28}

Microwave heating can remarkably reduce synthesis time compared with conventional heating. In the synthesis of porous materials, it has been reported that the

microwave synthesis method could provide an efficient way to control particle size distribution, phase selectivity, and macroscopic morphology.

2.4 Catalytic synthesis of carbonates

There is an increasing trend to consider carbon dioxide as a raw material resource and a business opportunity rather than a waste with a cost of disposal. Increasing amounts of low-cost and relatively pure CO₂ will be soon available from plants for carbon sequestration and storage. Carbon dioxide represents potentially a feedstock of nearly zero or even negative cost for conversion to fuels and useful chemicals.

Cyclic carbonates are useful intermediates for electrolytes in lithium ion batteries, green solvents and polycarbonates.^{5,6} Currently, cyclic carbonate precursors are manufactured employing the highly toxic phosgene.⁶ An alternative and green approach for the synthesis of cyclic carbonates is the insertion reaction of CO₂ into an epoxide (Figure 5). This route represents a very useful approach to effectively use CO₂ for the conversion of chemicals. The commercial production of cyclic carbonates employs non-expensive catalysts like homogeneous quaternary ammonium salts.^{7,8} SAPO-56 displays both remarkably high CO₂ adsorption capacity and Bronsted acid sites associated with Al ions and Lewis acid sites associated with OH groups^{35d} in its framework. This promoted us to evaluate its catalytic performance in the cycloaddition of CO₂ to epichlorohydrin.

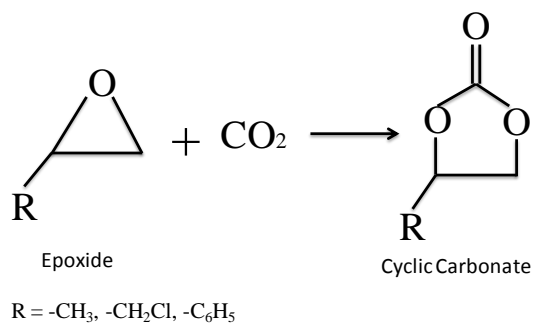


Figure 4 Schematic showing the catalytic conversion of CO₂ into a cyclic carbonate

The synthesis of cyclic carbonates from epoxides and carbon dioxide has been a commercial process since the 1950s⁹ and is now operated commercially by many different companies worldwide. The interest in cyclic carbonates is driven by their wide range of chemical and technological applications.¹⁰

CHAPTER 3 EXPERIMENTAL APPROACH

3.1 Synthesis of SAPO-56 crystals via hydrothermal synthesis

SAPO-56 crystals were synthesized hydrothermally following the synthetic procedure reported before ⁴⁴. In a typical synthesis, shown in Figure 5, a solution of orthophosphoric acid (85% wt.%, Sigma-Aldrich) deionized water, and aluminium hydroxide (76.5% min, Alfa Aesar) was vigorously stirred for ~1 hour. To this solution, Ludox AS-40 colloidal silica (40 wt.%, Sigma-Aldrich) and N,N,N',N'-tetramethylhexane-1,6-diamine (TMHD, Aldrich) were added. The resultant solution was stirred for 24 hours at room temperature. The gel composition was: 2.0 TMHD: 0.6 SiO₂: 0.8 Al₂O₃: P₂O₅: 40H₂O. The resultant gel was transferred into a 50 mL Teflon vessel. The vessel was placed into the stainless- steel autoclave, Figure 7, to allow the solution to reach an autogeneous pressure as heated. The autoclave was placed into an oven, Figure 8, at 200 °C for 96 hours. Then, the autoclave was cooled down and the solid product was recovered by centrifugation at 3000 rpm, Figure 9, and washed three times with deionized water and dried at 100 °C overnight. The resulting crystals was calcined in a programmable oven, Figure 10, with heating rate of 1 °C/min and cooling rate of 5 °C/min from room temperature to 400 °C for 20 hours.

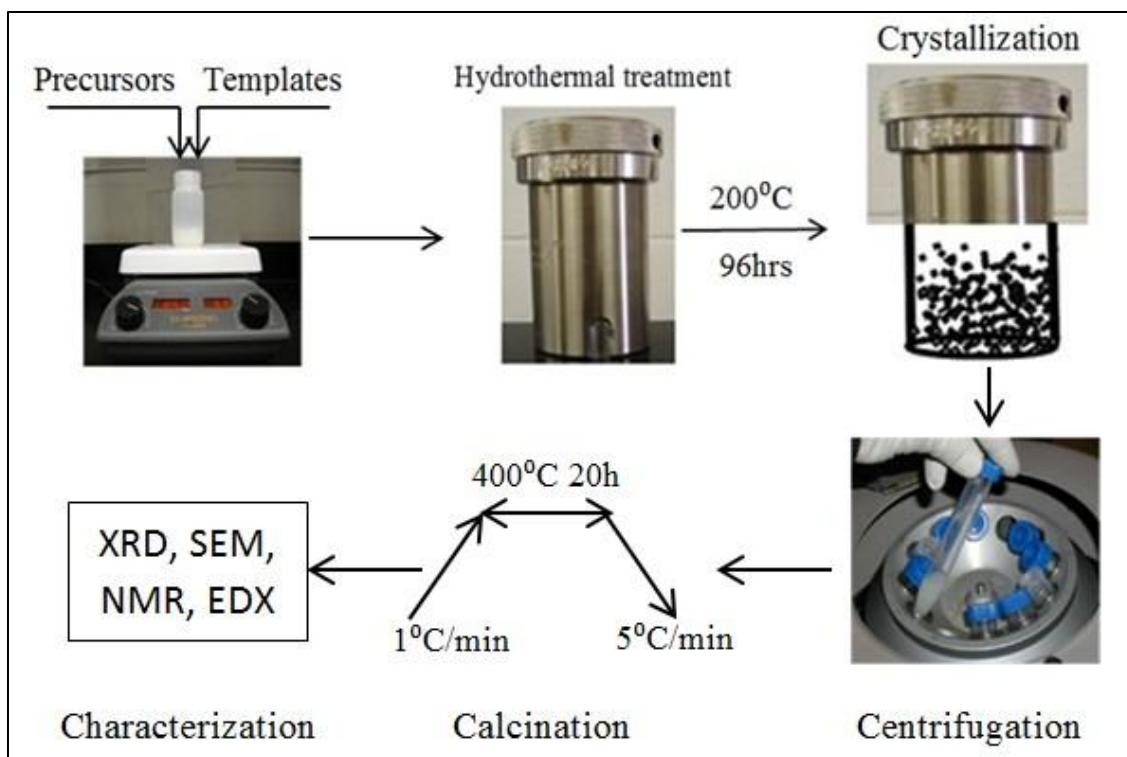


Figure 5 SAPO-56 crystals synthesis procedure using hydrothermal method

3.2 Synthesis SAPO-56 via microwave approach

The hydrothermal synthesis approach used to synthesize SAPO-56 requires typically long synthesis times (days) and relatively high hydrothermal temperatures (200 °C). Microwave (MW) heating offers several advantages over conventional heating, such as fast crystallization, phase selectivity, narrow particle size distribution, abundant nucleation, morphology and size control and rapid and uniform heating.

The gel required for synthesizing SAPO-56 crystals via MW was prepared the same with hydrothermal approach, Figure 6. The resultant solution was stirred for 24 hours at room temperature. The homogeneous gel was transferred to a glass tube and MW heating for different times was carried out with continuous stirring in a computer controlled MW

oven (Mars 5, CEM corp., frequency of $\sim 10^{10}$ Hz), (Figure 11), at 150 °C and 250 psi. After cooling, the product was separated using centrifugation for 3 times (each for 20 min at 3000 rpm) and dried overnight at 60 °C. The as-synthesized crystals were calcined at 400 °C for 20 hours at 1 °C/min and 5 °C/min heating and cooling rates respectively to remove the organic template.

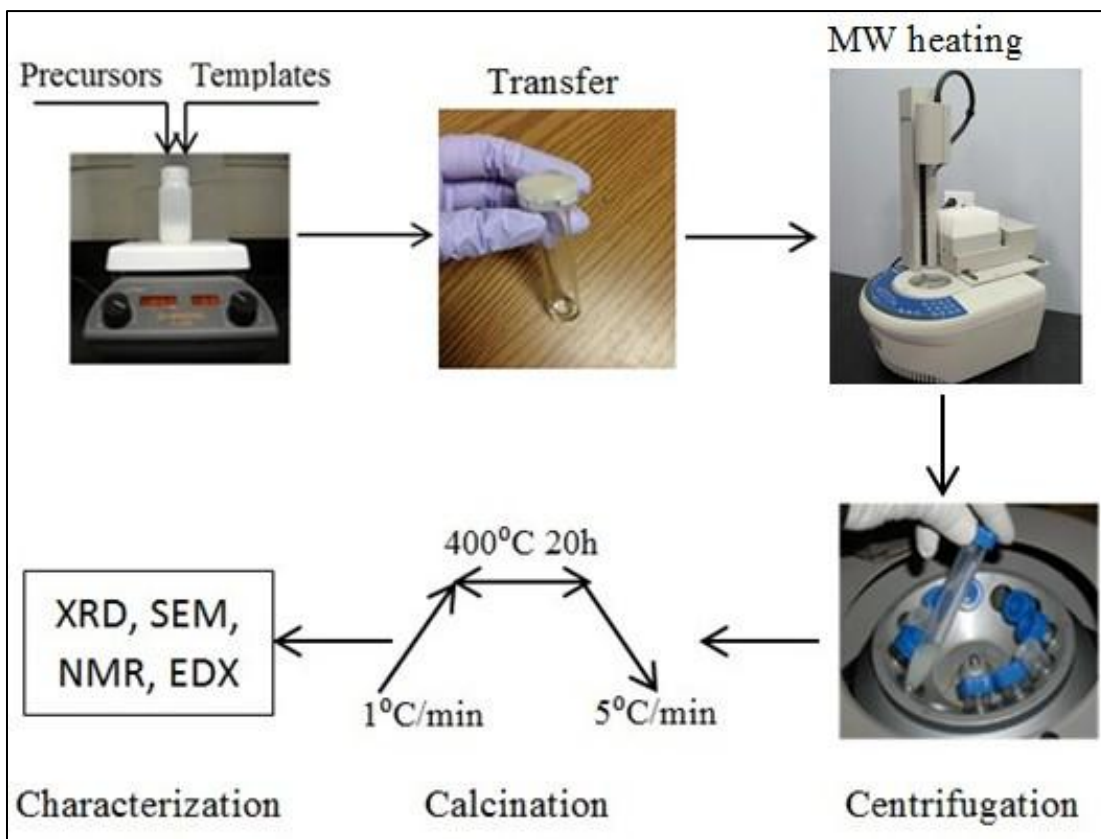


Figure 6 SAPO-56 crystal syntheses via MW

3.3 Characterization

The resulting crystals were then characterized using X-ray diffraction, scanning electron microscopy, transmission electron microscopy and adsorption isotherms. The morphology of the crystals was determined with a FE-SEM (FEI Nova 600), Figure 13, with an acceleration voltage of 6 kV. Powder X-ray diffraction patterns were collected

using a Bruker D8-Discover diffractometer, Figure 14, at 40 kV, 40 mA with Cu K α radiation. Transmission electron microscopy (TEM) studies, including TEM imaging, selected area electron diffraction (SAED), and energy-dispersive x-ray spectroscopy (EDS), were performed using a FEI Tecnai F20 transmission electron microscope. A field emission gun (FEG) was used for the electron source and the studies were performed at the accelerating voltage of 200 keV. Carbon dioxide adsorption isotherms were collected using a Micromeritics Tristar 3000 porosimeter, Figure 15, at room temperature employing water as coolant. Prior to the measurements, the samples were degassed at 150 °C for ~3 hours.

The acidic properties of the MW SAPO-56 were determined using NH₃ as a probe molecule. In temperature-programmed desorption of ammonia (NH₃-TPD; Micromeritics Auto Chem 2910 instrument, Figure 16), 0.1 g of the catalyst was taken in a U-shaped, flow-through, quartz sample tube. Prior to measurements, the catalyst was pretreated in He (30 ml/min) at 250 °C for 1 hr. A mixture of NH₃ in He (10 vol%) was passed (30 ml/min) at 50 °C for 1 hr. The sample was, then, flushed with He (30 ml/min) for 1 hr. TPD measurements were carried out by raising the temperature from 100 to 500 °C at a heating rate of 5 °C/min. From the areas of the desorption peaks and from the calibration curves generated prior to the analyses of the catalyst samples, the amount of acid sites present in the catalysts were determined.

The solid-state NMR (nuclear magnetic resonance) spectra were recorded at room temperature and ambient pressure on a Tecmag Discovery spectrometer (Varian 7600 AS

400 MHz), using a Doty Scientific magic angle-spinning (MAS) probe with 7 mm (outside diameter) sapphire rotors, Figure 17.

Cross-polarization with MAS (CP-MAS) was used to acquire ^{29}Si data at 59.622 MHz. The ^1H ninety-degree pulse width was 3.7 μs . The mixing time was 1.5 ms. The MAS sample spinning rate was 2.5 kHz or 4 kHz. Recycle delay between scans was 2 s with the acquisition time to be 20.48 ms, determined by observing no apparent loss in the ^{29}Si signal from one scan to the next. The ^{29}Si chemical shifts are given relative to hexamethylcyclotrisiloxane ($[(\text{CH}_3)_2\text{SiO}]_3$) as secondary reference, which has a chemical shift to be 9 ppm calibrated using the ^{29}Si signal of TMS assigned to zero ppm.

For one pulse experiments, the ^{29}Si data was also acquired at 59.622 MHz. The ^{29}Si pulse width was 1.5 μs , and the delay time was 30 s. The spinning rate of the rotors was either 2.5 kHz or 3.0 kHz, depending upon the stability of the rotation. All the other parameters were the same as CP-MAS experiments.

3.4 SAPO-56 catalyzed CO_2 conversion to carbonates

The catalytic activity of SAPO-56 was evaluated in the cycloaddition of CO_2 to epichlorohydrin to form chloropropene carbonate. In a typical cycloaddition reaction, 18 mmol of epichlorohydrin and 100 mg of SAPO-56 were placed in a 250 ml stainless steel high pressure Parr reactor (Model 4576A), Figure 12. The reactor was pressurized with CO_2 at 10 bar, and the reaction was carried out under stirring at different temperatures for 4 hr. After the reaction, the reactor was cooled to room temperature, the unreacted CO_2

was vented out, the catalyst was separated by centrifugation, and the products were analyzed by ^1H NMR spectrometry.

3.5 Equipment

The following equipment was used for the hydrothermal synthesis of SAPO-56: hydrothermal synthesis autoclaves (Figure 7) and oven (Figure 8). For the MW synthesis (Figure 11); reaction of the cyclic carbonate (Figure 12). The instrumentation needed for characterizing SAPO-56 is shown in Figure 13 to 17.

3.5.1. Hydrothermal synthesis of SAPO-56



Figure 7 Hydrothermal Autoclave with 50mL Teflon Vessel³⁶



Figure 8 Hydrothermal Synthesis oven



Figure 9 Eppendorf Centrifuge
Model No:5702
Series No: 5702YN320989



Figure 10 Programming oven

Ney® Vulcan 3-550 Furnace
Dentsupply Ceramco International
Serial No.: 9493308
York, PA 17404³⁷



Figure 11 Microwave instrument
Mars 5, CEM corp.

3.5.2. Reaction



Figure 12 Parr Reactor Model 4576A

3.5.3. SAPO-56 Characterization



Figure 13 Nova Nano SEM 600

FEI³⁸



Figure 14 X-Ray Diffraction
Bruker AXS – Diffraktometer D8
Serial No.: 203407
Karlsruhe, Germany D76181

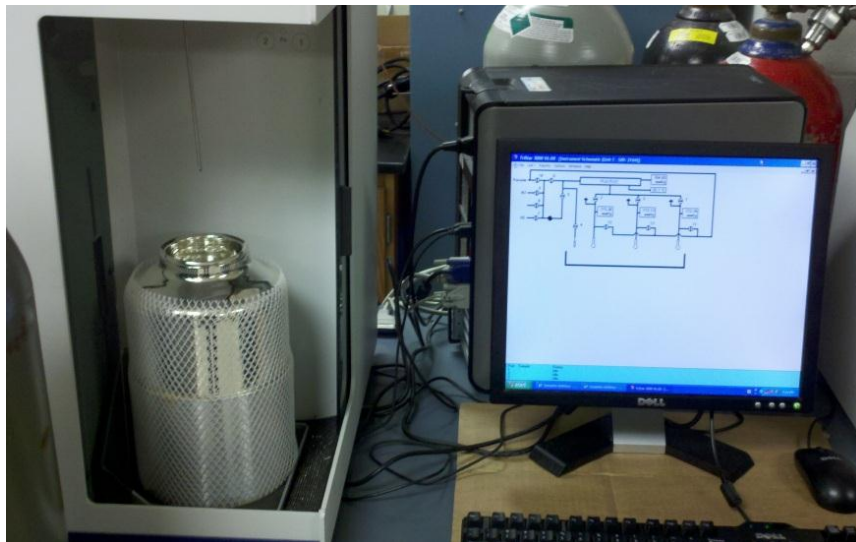


Figure 15 Micromeritics Tristar 3000 Porosimeter



Figure 16 Micromeritics Autochem 2910



Figure 17 NMR

CHAPTER 4 RESULTS AND DISCUSSION

4.1 Characterization of SAPO-56

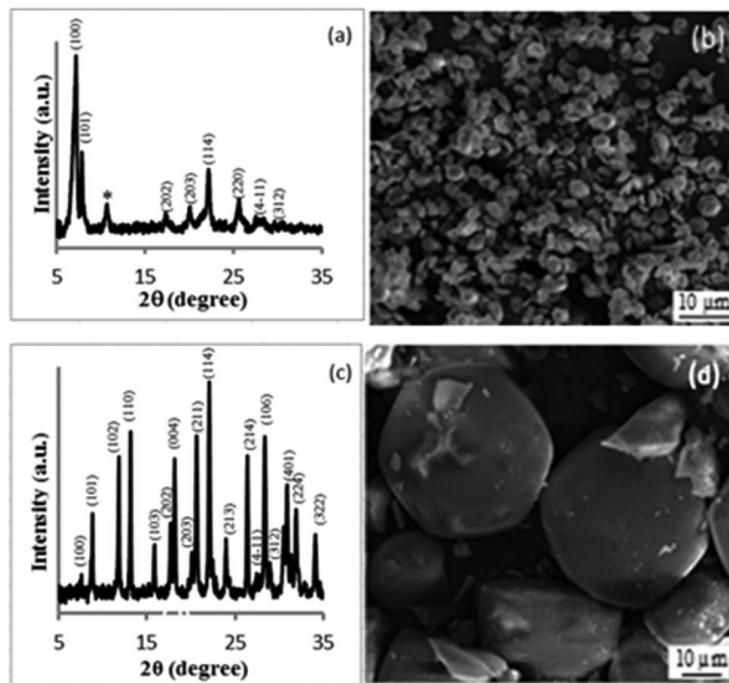


Figure 18 (a) XRD pattern and (b) SEM image of SAPO-56 crystals synthesized via microwave heating at 150 °C and 250 psi for 10 minutes. *Denotes SAPO-17. (c) XRD pattern and (d) SEM image of SAPO-56 crystals synthesized via conventional hydrothermal treatment. The same gel composition was used for both samples.

Figure 18a shows the XRD pattern of SAPO-56 crystals synthesized via MW for 10 minutes at 150 °C. All the peaks (but one at an interplanar spacing of ~ 8.9 Å) correspond to SAPO-56 with AFX topology and are in good agreement with the reported literature.³⁵ A secondary reflection at d spacing ~ 9 Å was assigned to SAPO-17 (ERI topology).^{35d, 39} We estimated the % of SAPO-17 for this particular sample to be $\sim 15\%$

(from radial intensity distribution profiles).

In all microwave assisted synthesis, SAPO-17 coexisted as a secondary phase. The coexistence of these two zeolite phases has been previously observed.^{35a} Both zeolite phases are prepared with the same structure directing agent, and therefore the coexistence of both topologies has been associated with changes in silica, and template concentrations^{35a} as the hydrothermal synthesis progresses. It is likely that longer synthesis times resulted in a change in concentration of the template favoring the formation of SAPO-17 over SAPO-56. In addition, it is well known that zeolite synthesis is governed by the occurrence of successive phase transformations. Thermodynamically, the least favorable phase crystallizes first, and is replaced by more stable phases.⁴⁰ Our results suggest that under the employed MW experimental conditions, SAPO-17 is the most thermodynamically stable phase. The morphological features of the MW synthesized SAPO-56 crystals revealed homogeneous hexagonal crystals of ~3-4 μm as shown in Figure 18b. For comparison, SAPO-56 was prepared by a conventional hydrothermal synthesis approach at 200 °C (Figure 18c) for 96 hours. Large hexagonal crystals of ~50 micron size were observed (Figure 18d).

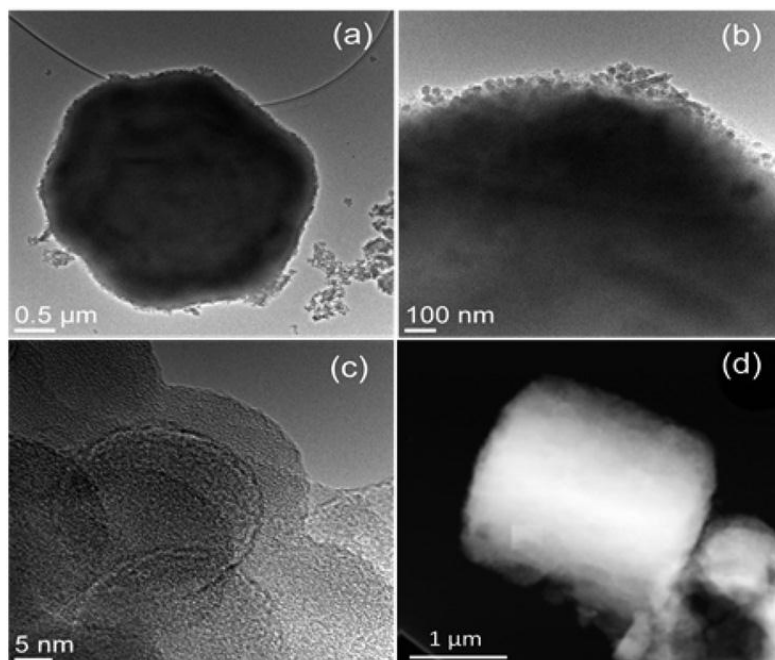


Figure 19 HRTEM of (a) hexagonal SAPO-56 crystals synthesized via microwave heating at 150 °C and 250 psi for 10 minutes, (b) silica nanospheres present at the surface of the SAPO-56 crystals, (c) higher magnification of the ~25 nm silica nanospheres, (d) rod-like crystals corresponding to SAPO-17.

Transmission electron microscopy and selected area electron diffraction (SAED) were used to confirm the morphology and crystal structure of SAPO-56. Figure 19 shows TEM micrographs of representative crystals observed in the MW synthesized sample. In agreement with the SEM study, most of the crystals showed hexagonal morphology and their sizes were in the ~3-4 μm range (Figure 19a). Nanospheres consisting of silica, as confirmed by EDS analysis, were observed on the surface of many crystals present in this sample (Figure 19b). A high-resolution TEM image of few such nanospheres is shown in Figure 19c. Their occurrence on the surface of SAPO-56 crystals suggests that not all the silica source (Ludox) reacted, which is reasonable based on the very short MW synthesis time (10 minutes). Few rod-like crystals were observed in this sample as shown in Figure 19d. This morphology has been associated with SAPO-17.^{35d} Within the experimental error of the EDS analysis, the measured elemental composition of hexagonal and rod-like

crystals was in agreement with nominal compositions of SAPO-56 and SAPO-17, respectively. It is important to mention that EDS distribution analysis shows that in the MW sample silicon was partially incorporated into the SAPO-56 framework (Figure 20), supporting the presence of silica nanospheres in the surface of SAPO-56 crystals.

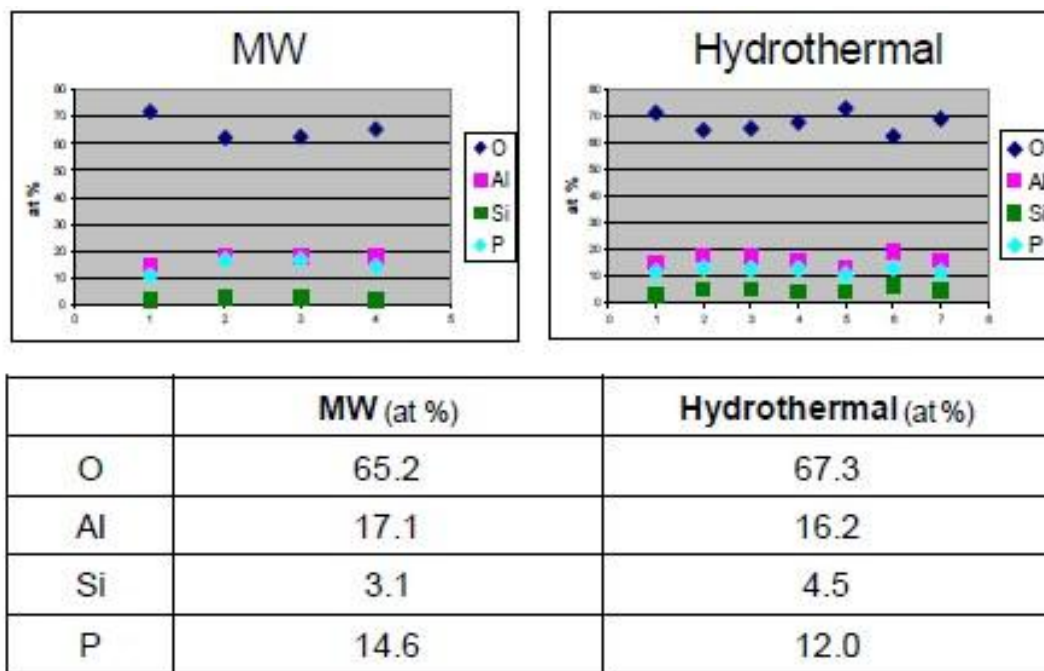
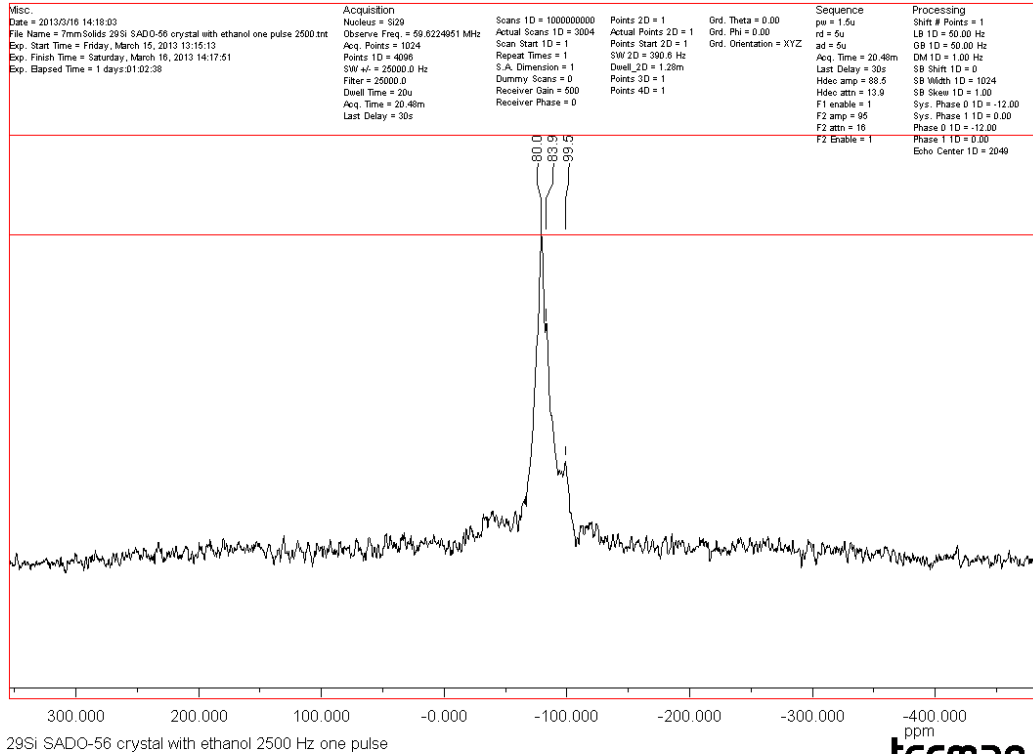
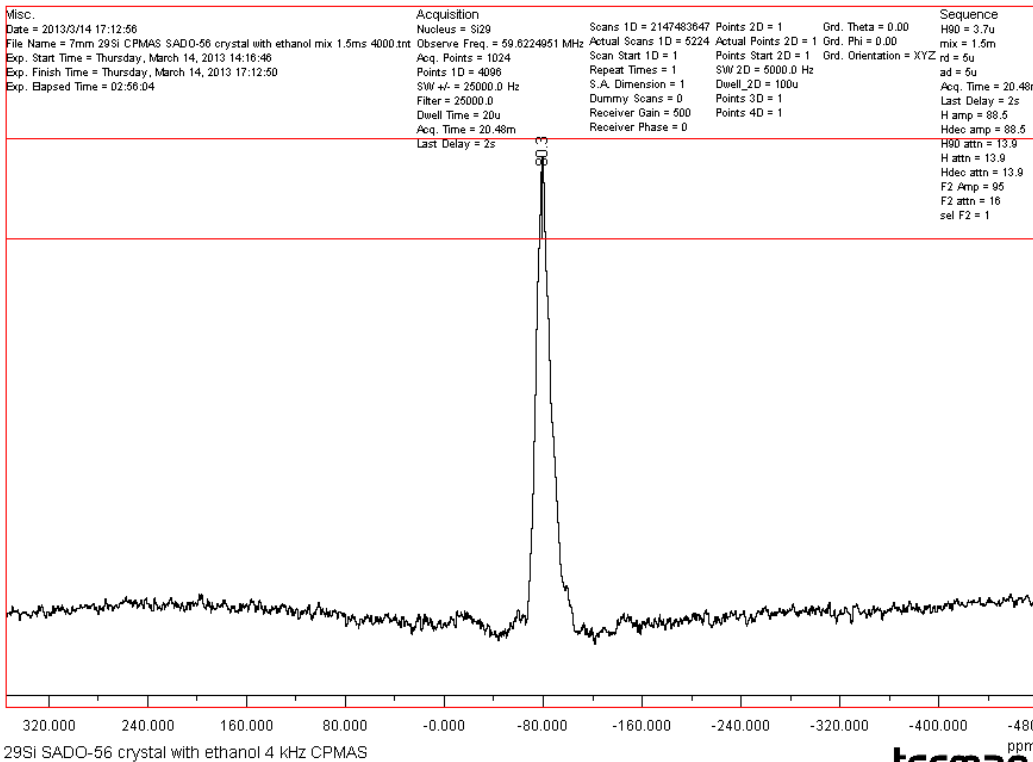


Figure 20 EDS distribution analysis for MW and hydrothermal synthesized samples.

^{29}Si NMR for the MW and hydrothermal synthesized samples are shown in Figure 21. A strong resonance at ~ -80 ppm is present for both samples. In addition for the MW sample two peak resonances are evident at -83.9 and -99.5 ppm.



tecmaq
TECHNOLOGY FOR MAGNETIC RESONANCE



tecmaq
TECHNOLOGY FOR MAGNETIC RESONANCE

Figure 21 ^{29}Si NMR of (a) MW synthesized and (b) hydrothermally synthesized SAPO-56.

Typical SAED ring patterns obtained from SAPO-56 crystals synthesized via MW are shown in Figure 22 (left). In order to measure all represented d-spacings, radial intensity distribution profiles were extracted from these SAED patterns. As shown in Figure 22 (right), both profiles reveal peaks at the same d-spacing values and they were found to be in agreement with the database XRD pattern of SAPO-56 (except for the reflection at ~ 8.9 Å, which is associated with SAPO-17).

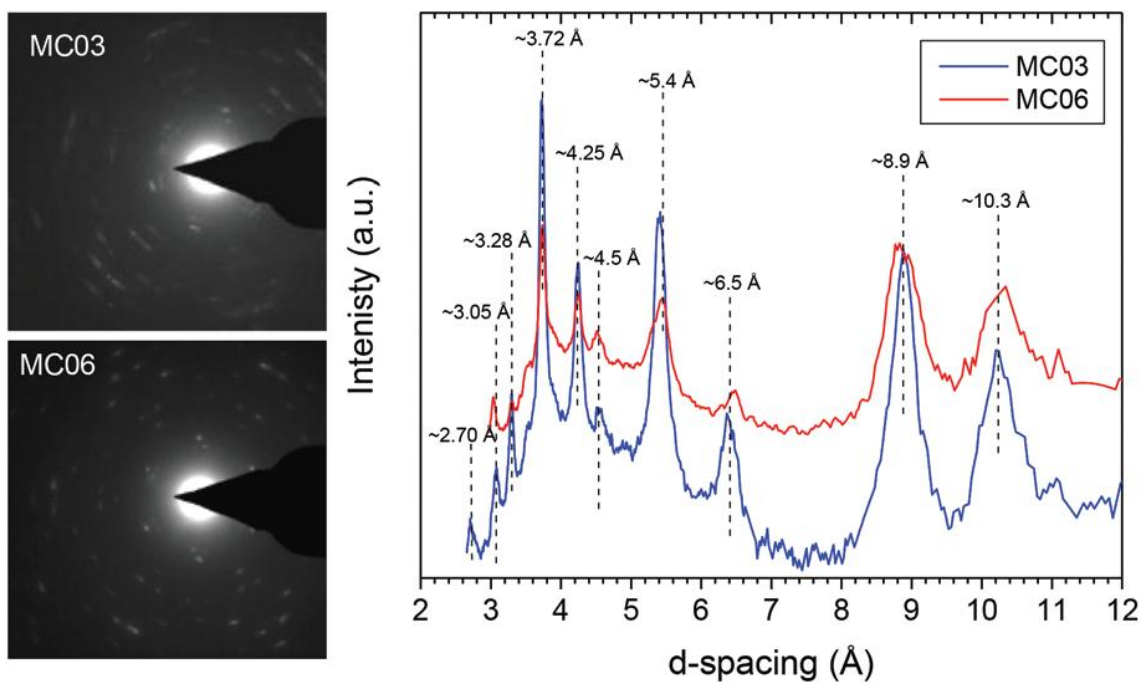


Figure 22 SAED patterns (left) and radial intensity distribution profiles (right) of SAPO-56 crystals synthesized via microwave heating at 150 °C and 250 psi for 10 minutes. MC03 and MC06 refer to two different analyzed micro-crystals.

Figure 23 shows that longer MW synthesis times led to a mixture of SAPO-56 and SAPO-17.

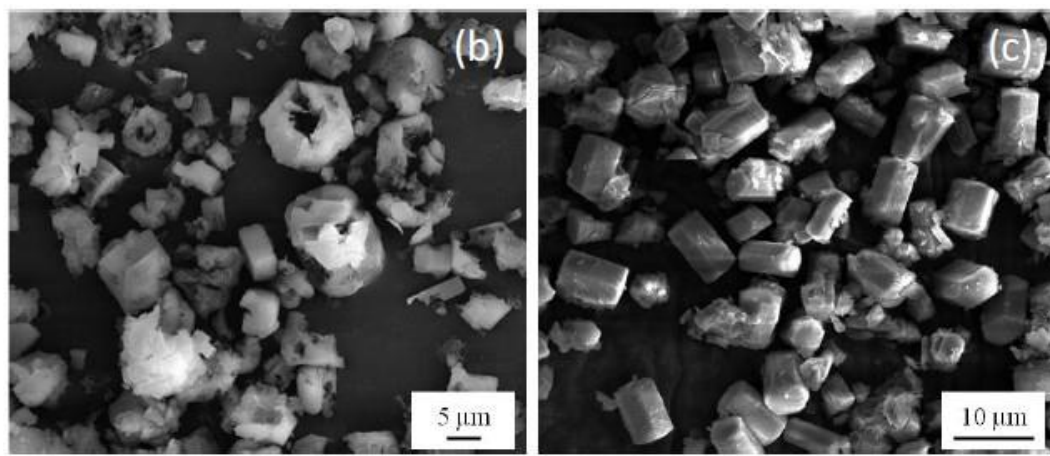
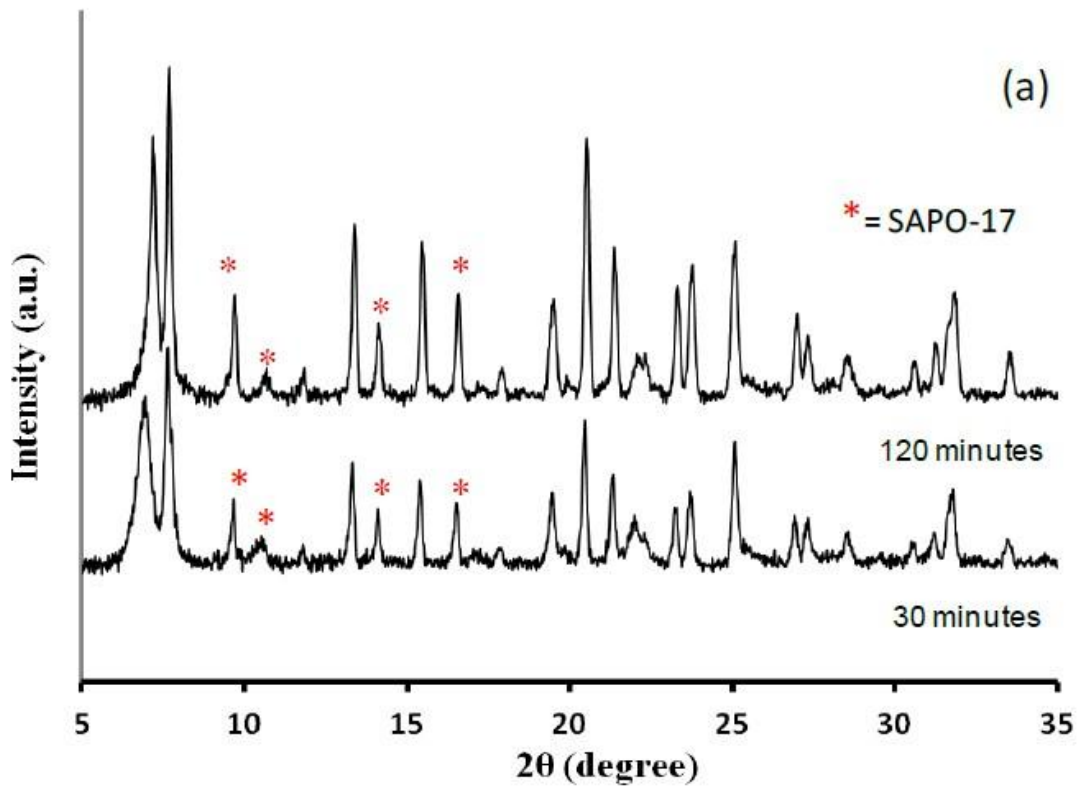


Figure 23 (a) XRD patterns of MW heated synthesized SAPO-56 crystals at 30 minutes and 120 minutes. Representative SEM images of the sample synthesized at (b) 30 minutes and (c) 120 minutes.

4.2 Catalytic activity

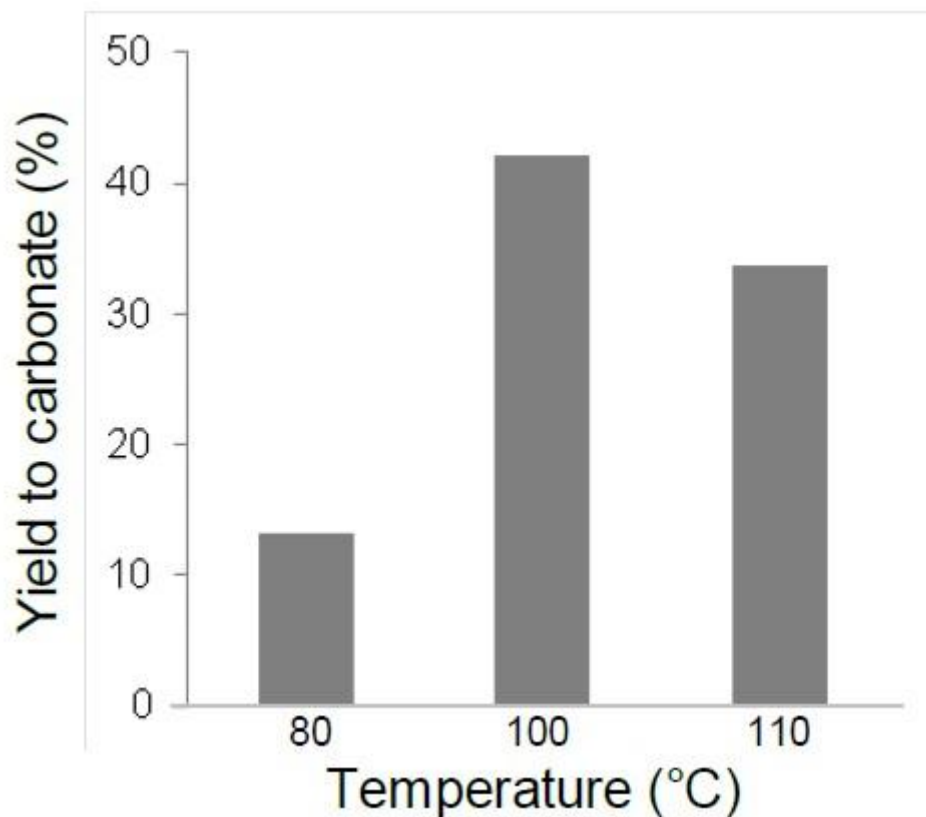


Figure 24 Yield to chloropropene carbonate at different temperature for hydrothermal synthesized SAPO-56.

Figure 24 shows the yield to chloropropene carbonate as a function of temperature for hydrothermal synthesized SAPO-56. The optimum temperature (100 °C) was chosen to test the catalytic activity of the MW sample.

The cycloaddition of CO₂ to epichlorohydrin yielded chloropropene carbonate as the main product, and diols and dimers of epichlorohydrin as minor products. Controlled experiments under our reaction conditions confirmed that the reaction did not proceed to a significant extent in the absence of the SAPO-56 catalyst. The yield to chloropropene carbonate was calculated by using ¹H NMR spectra, from signs obtained at chemical shifts of 4.54 ppm (¹H from chloropropene carbonate), 3.17 ppm (¹H from epichlorohydrin) and 3.9 ppm (¹H from the by-product 3-chloro-1,2-propanediol). GC-

MS (HP 5890 Gas chromatograph equipped with 5970 Mass Selective Detector; 30 m×0.32 mm column, HP-5 coated with 5% phenyl methyl poly siloxane stationary phase) was employed to confirm the presence of chloropropene carbonate, epichlorohydrin, and diol.

Table 1 Selected properties and catalytic performance of SAPO-56 in the cycloaddition of CO₂ to epichlorohydrin

Synthesis method ^a	Particle size (μm)	CO ₂ uptake (mmol/g) ^b	Yield to chloropropene carbonate(%)
Microwave	3-4	6.1	84.8
Hydrothermal	50	4.2	42.2

^a The same gel composition for both methods was used. ^b At 400 Torr. Reaction conditions: 100 °C; 4 h; CO₂ pressure= 10 bar; 100 mg catalyst; 18 mmol of epichlorohydrin.

Table 1 summarizes the catalytic performance of SAPO-56 crystals prepared via MW heating vs SAPO-56 prepared via conventional hydrothermal treatment in the cycloaddition of CO₂ to epichlorohydrin at 100 °C for 4 hr. The yield of chloropropene carbonate over the hydrothermally treated sample was 42.2%. For the MW heated sample the yield increased considerably to 84.8%. For the MW sample, when the reaction time was decreased to 2 hr, the yield of carbonate was only ~48%. Longer reaction times (i.e. 8 hr) promoted the polymerization of the product. The enhanced catalytic performance of the SAPO-56 crystals prepared via a MW assisted approach as compared to the hydrothermally synthesized crystals in the cycloaddition of CO₂ to epichlorohydrin may be related to the smaller crystal size with narrow particle size distribution and higher CO₂ uptakes (Figure 25). In fact, the yield of chloropropene carbonate correlate with CO₂

uptake (Figure 26). High CO₂ adsorption capacities promote the catalytic conversion of CO₂ to cyclic carbonates.⁴¹ ZIF-8 and Cu-MOF are metal organic frameworks that were also active for this particular reaction.

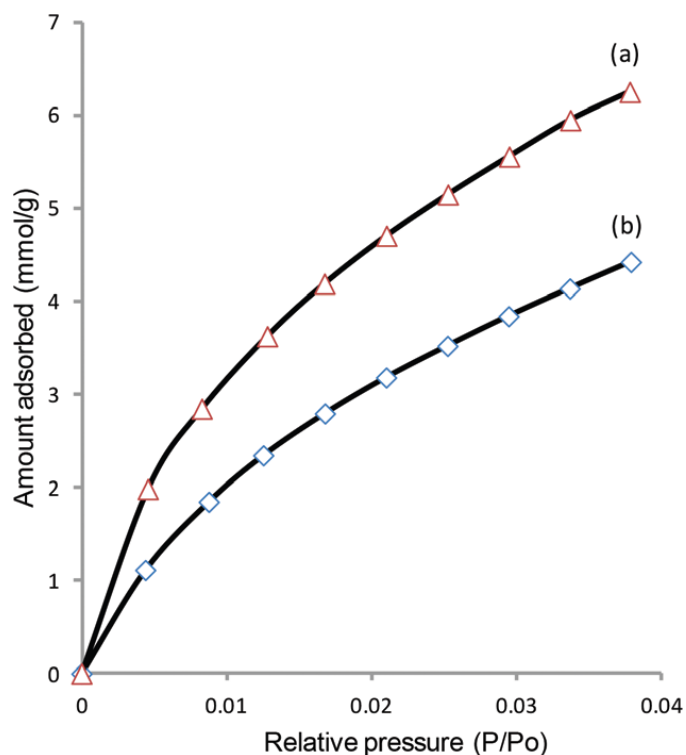


Figure 25 CO₂ uptakes for SAPO-56 crystals synthesized via (a) microwave assisted approach and (b) hydrothermal treatment.

The higher conversion of microwave sample may be also related with the presence of SAPO-17, with ERI as its topology. The pore size of SAPO-17 ($\sim 3.6 \times 5.1$ Å) is much larger, so this may promote the conversion of CO₂ to carbonate. On the other hand, the CO₂ uptakes for SAPO-17 are much lower than SAPO-56, which is not the prerequisite of higher conversion. So we think the higher conversion of CO₂ is mainly due to the SAPO-56.

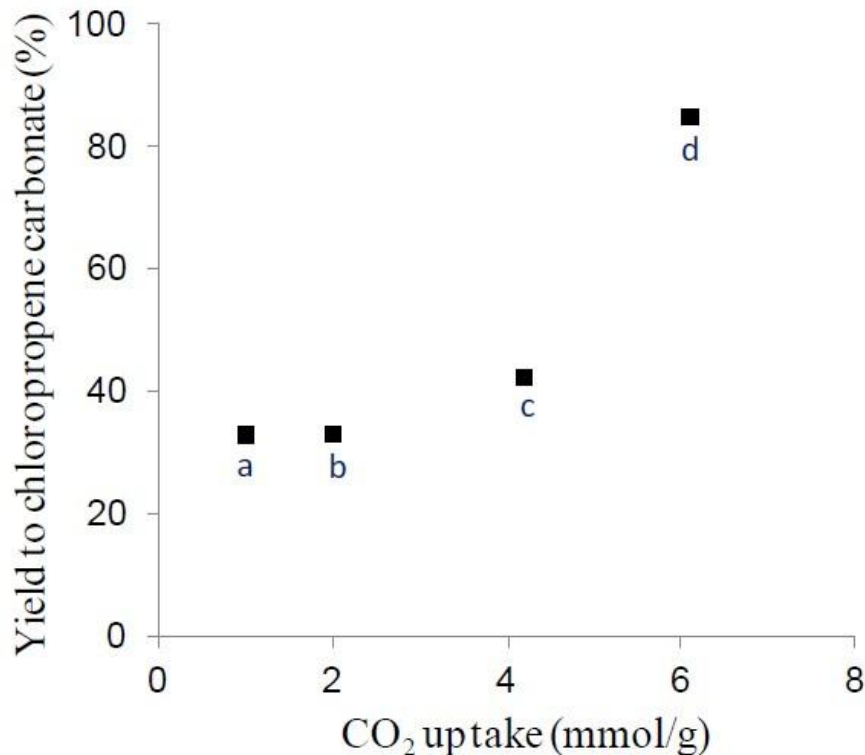


Figure 26 Correlation between Yield to chloropropene carbonate (%) and CO₂ uptake for different catalysts: (a) ZIF-8, (b) Cu-MOF, ⁴² (c) SAPO-56 (HT), (d) SAPO-56 (MW). Reaction conditions for all catalysts: 100 °C, 4 hr, 18 mmol of epichlorohydrin and 100 mg of catalyst. CO₂ uptakes taken at 400 Torr.

NH₃ TPD was used to identify and quantify the concentration of acid sites of the MW and hydrothermal synthesized SAPO-56 crystals. The TPD results for the MW sample showed two desorption peaks with a peak maximum at 198 °C and 483 °C (Figure 27). The concentration of acid sites was estimated using the total area under the curve for the two desorption peaks, and corresponded to 1.240 mmol g⁻¹. For the hydrothermally synthesized sample two desorption peaks with peak maxima at 204 °C and 496 °C were observed, corresponding to a concentration of acid sites of 1.701 mmol g⁻¹. The lower concentration of acid sites in the MW sample may be related to the presence of the silica (neutral) nanospheres in the surface.

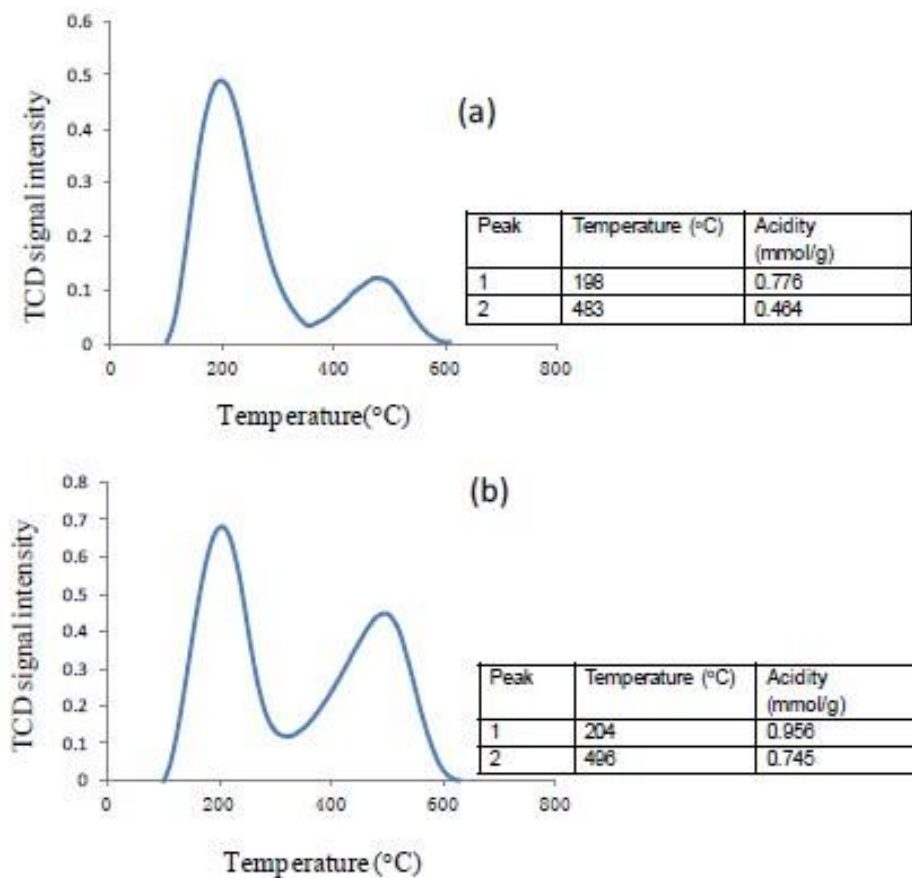


Figure 27 NH₃-TPD of (a) MW synthesized and (b) hydrothermally synthesized SAPO-56.

The silica nanospheres can be visualized as defects, and may play a role as specific surface sites for the cycloaddition reaction. Recycle experiments were carried out to assess the stability of the catalysts. In the recycle experiments, the catalysts after use in the cycloaddition reaction were washed thoroughly with acetone, centrifuged and air dried before reuse. There were no evident changes in catalytic activity for both catalysts. The stability of other zeolite based compositions for cycloaddition reactions is well known.⁴³

CHAPTER 5 CONCLUSIONS

1. The synthesis of SAPO-56 crystals via microwave heating was demonstrated.
2. In contrast to hydrothermal synthesized crystals, the microwave synthesized crystals displayed smaller crystal sizes (3-4 μm) with narrow size distribution and were prepared in shorter synthesis times (10 minutes) and lower temperatures (150 $^{\circ}\text{C}$). Longer microwave synthesis time leads to the coexistence of SAPO-56 and SAPO-17.
3. The resultant SAPO-56 crystals from microwave displayed high catalytic activity in the synthesis of chloropropene carbonate from CO_2 and epichlorohydrin (84.8%) compare to hydrothermal treatment.
4. The enhanced catalytic activity of SAPO-56 crystals was related to its high CO_2 adsorption capacity, small crystal size, and the presence of acid sites in their framework known to be active sites in cycloaddition reactions.

CHAPTER 6 FUTURE DIRECTIONS

Our results demonstrated the synthesis of SAPO-56 crystals by microwave process. In the reaction of CO₂ and epichlorohydrin to carbonate, the MW-assisted crystals displayed higher catalytic activity than hydrothermal-assisted crystals. Future work can focus on the reaction of CO₂ with other epoxides, such as styrene oxide, propene oxide to obtain others carbonates by using the MW-synthesized SAPO-56 crystals. In the MW experiment, the tube we used was very small so it produced very small amount of SAPO-56 crystals by one time. So in the future, we can improve our experiment to get more crystals by changing a large container. In that case, the large amount of catalysts can meet the industry requirements. In addition, SAPO-56 can be also an effective catalyst for the synthesis of carbamate via the catalytic conversion of CO₂ and amines.

As we know, the pore size of SAPO-56 is $\sim 3.4 \times 3.6$ Å, CO₂ is 3.3 Å and the pore size of CH₄ is 3.8 Å, so in this respect SAPO-56 is of great interest in membrane technology. Zeolite membranes can effectively separate CO₂ from light gases, which is really important both in the environmental and energy perspective. In the future, SAPO-56 membranes can be synthesized for gas mixture separation.

REFERENCES

1. Emissions of Greenhouse Gases in the United States, Energy information Administration, Report # DOE/ EIA-0573 (2007), **2007**
2. Boden, T. A.; Marland, G. and Anders, R.J.; Global, Regional, and National Fossil-Fuel CO₂ emissions.
3. Orr, Jr., F. M.; *Energy Environ. Sci.* **2009**, *2*, 449.
4. Schrag, D.P.; *Science* **2007**, *315*, 812.
5. McKetta, J.J.; Cunningham, W.A.; *Encyclopedia of Chemical Processing and Design*, **1984**, *20*, 177.
6. Behr, A., *Angew Chem Int Ed*, **1988**, *27*, 661.
7. Fukuoka, S.; Kawamura, M.; Komiya, K.; Tojo, M.; Hachiya, H.; Hasegawa, K.; Aminaka, M.; Okamoto, H.; Fukawa, I.; Konno, S.; *Green Chem*, **2003**, *5*, 497.
8. *Filtrat Ind Anal*, **1999**, *27*, 2.
9. Peppel, W.J., *Ind Eng. Chem.*, **1958**, *50*, 767.
10. Schaffner, B.; Schaffner, F.; Verevkin, S.P.; Borner, A.; *Chem. Rev.* **2010**, *110*, 4554.
11. Byrappa, K.; Yoshimura, M.; *Handbook of Hydrothermal Technology* (Noyes Publications/William Andrew Publishing LLC, U.S.A. 2001).
12. Roy, R.; *Journal of Solid State Chemistry*, **1994**, *111*, 11.
13. Sômiya, S.; *Hydrothermal Reactions for Materials Science and Engineering. An Overview of Research in Japan* (Elsevier Science Publishers Ltd., U.K. **1989**).
14. Yoshimura, M.; Suchanek, W. L.; Byrappa, K.; *MRS Bulletin*, **2000** *25*, 17.
15. Gersten, B.; Lencka, M.; Riman, R. E.; *Chemistry of Materials*, **2002**, *14*, 1950.
16. Riman, R. E.; in *High Performance Ceramics: Surface Chemistry in Processing Technology*, edited by R. Pugh and L. Bergström (Marcel-Dekker, U.S.A. **1993**), 29.
17. Tosheva, L.; Valtchev, V. P. *Chem. Mater.* **2005**, *17*, 2494
18. Botella, P.; Corma, A.; Iborra, S.; Monton, R.; Rodriguez, I.; Costa, V.J. *Catal.* **2007**, *250*, 161.
19. Waller, P.; Shan, Z.; Marchese, L.; Tartaglione, G.; Zhou, W.; Jasen, J.C.; Maschmeyer, T. *Chem.sEur. J.* **2004**, *10*, 4970.
20. Li, Y.; Yang, W.; *Journal of Membrane Science*, **2008**, *316*, 3.
21. Chu, P.; Dwyer, F. G.; Vartuli, J. C.; *US Patent 4*, **1988**, 778, 666,
22. Heyden, H. V.; Mintova, S.; Bein, T.; "Nanosized SAPO-34 Synthesized from Colloidal Solutions" *Chem. Mater.*, **2008**, *20*, 2956.
23. Yang, W.; Zhang, B.; Liu, X.; "Synthesis and characterization of SAPO-5 membranes on porous α -Al₂O₃ substrates" *Micro. Meso. Mater.* **2009**, *117*, 391.
24. Kumar, N.; Villegas, J.I.; Salmi, T.; Murzin, Y.D.; Heikkila, T.; "Isomerization of n-butane to isobutene over Pt-SAPO-5, SAPO-5, Pt-H-mordenite and H-mordenite catalysts" *Catal. Today*. **2005**, *100*, 355.

25. Carreon, M.A.; Li, S.; Falconer, J.L.; Noble, R.D. "SAPO-34 Seeds and Membranes Prepared Using Multiple Structure Directing Agents" *Adv. Mater.* **2008**, *20*, 729.
26. Tosheva, L.; Ng, E. P.; Mintova, S.; Holzl, M.; Metzger, T.H.; Doyle, A.M. "AlPO₄-18 Seed Layers and Films by Secondary Growth" *Chem. Mater.* **2008**, *20*, 5721.
27. Cundy, C.S. "Microwave Techniques in the Synthesis and Modification of Zeolite Catalysts: A Review." Collection of Czechoslovak, *Chem. Comm.* **1988**, *63*, 1699.
28. Tompsett, G.A.; Conner, W.C. "Microwave Synthesis of Nanoporous Materials" *Chem. Phys. Chem.*, **2006**, *7*, 296.
29. Szostak, R.; Molecular Sieves: Principles of Synthesis and Identification, Van Nostrand Reinhold, New York, **1989**.
30. Terres, E.; Influence of the Synthesis Parameters on Textural and Structural Properties of MCM-41 Mesoporous Material, *Microporous and Mesoporous Materials*, **1996**, *431*, 111.
31. Boukadir, D.; Bettahar, N.; Derriche, Z.; Synthesis of zeolites 4A and HS from natural materials, *Annales de Chimie - Science des Materiaux*, **2002**, *27*, 1.
32. (a) Carreon, M.A.; Li, S.; Falconer, J.L.; Noble, R.D.; *J. Am. Chem. Soc.*, **2008**, *130*, 5412; (b) Carreon, M.A.; Li, S.; Falconer, J.L.; Noble, R.D.; *Adv. Mater.*; **2008**, *20*, 729; (c) Li, S.; Falconer, J.L.; Noble, R.D.; *Microporous Mesoporous Mater.*; **2008**, *110*, 310; (d) Hong, M.; Li, S.; Falconer, J.L.; Noble, R.D.; *J. Membr. Sci.*, **2008**, *307*, 277; (e) Yang, W.; Zhang, B.; Liu, X.; *Microporous Mesoporous Mater.*; **2009**, *117*, 391; (f) Ciobanu, G.; Carga, G.; Ciobanu, O.; *Desalination*, **2008**, *222*, 197; (g) Venna, S.R.; Carreon, M.A.; *Langmuir*, **2011**, *27*, 2888.
33. (a) Zhou, H.; Wang, Y.; Wei, F.; Wang, D.; Wang, Z.; *Appl. Catal. A*, **2008**, *348*, 135; (b) Zhou, H.; Wang, Y.; Wei, F.; Wang, D.; Wang, Z.; *Appl. Catal. A*, **2008**, *341*, 112; (c) Wei, Y.; Zhang, D.; Xu, L.; Chang, F.; He, Y.; Meng, S.; Su, B.L.; Liu, Z.; *Catal. Today*, **2008**, *131*, 262; (d) Roldan, R.; Sanchez, M.; Sankar, G.; Romero-Salguero, F.J.; Jimenez-Sanchidrian, C.; *Microporous Mesoporous Mater.*, **2007**, *99*, 288; (e) Kumar, N.; Villegas, J.I.; Salmi, T.; Murzin, Y.D.; Heikkila, T.; *Catal. Today*, **2005**, *100*, 355; (f) Liu, G.; Tian, P.; Li, J.; Zhang, D.; Zhou, F.; Liu, Z.; *Microporous Mesoporous Mater.*, **2008**, *111*, 143.
34. Denayer, J.F.M.; Devriese, L.I.; Couck, S.; Singh, R.; Webley, P.A.; Baron, G.V.; *J. Phys. Chem. C*, **2008**, *112*, 16593.
35. Wilson, S.T.; McGuire, N.K.; Blackwell, C.S.; Bateman, C.A.; Kirchner, R.M.; *Stud. Surf. Sci. Catal.* **1995**, *98*, 9; (b) Wilson, S.T.; Broach, R.W.; Blackwell, C.S.; Bateman, N.K.; Kirchner, R.M.; *Microporous Mesoporous Mater.* **1999**, *28*, 125; (c) Xu, R.; Pang, W.; Yu, J.; Huo, Q.; Chen, J.; *Chemistry of Zeolites and Related Porous Materials. Synthesis and Structure*, Wiley, **2007**, 45; (d) Cheung, O.; Liu, Q.; Bacsik, Z.; Hedin, N.; *Microporous Mesoporous Mater.* **2012**, *156*, 90; (e) Wilson, S.T.; *US Pat.* **5**, 370, 851, **1994**.
36. Group, N. Nanostructures Synthesis. <http://nanotubes.epfl.ch/page-24503-en.html>
37. Chong, N. Synthesis and Characterization of Ceria Nanomaterials. University of Louisville, **2010**.
38. Manufacturer Specifications - Nova NanoSEM 600, FEI. <http://www.medwow.com/med/scanning-electron-microscope/fei/nova-nanosem-600/33713.model-spec>.

39. Valyocsik, E.W.; Ballmoos, R. von; *US Pat.* 4, 778, 780, **1988**.
40. Kuanchertchoo, N.; Kulprathipanja, S.; Aungkavattana, P.; Atong, D.; Hemra, K.; Rirksomboon, T.; Wongkasemjit, S.; *Appl. Organomet. Chem.* **2006**, *20*, 721.
41. Ratnasamy, P.; Srinivas, D.; Handbook of Heterogeneous Catalysis, ed. Ertl, G.; Knozinger, H.; Schuth, F.; Weitkamp, J.; Wiley-VCH, New York, 2nd edn, **2008**, *7*, 3717.
42. (a) Miralda, C.; Zhu, M.; Macias, E.E.; Ratnasamy, P.; Carreon, M.A.; *ACS-Catalysis* **2012**, *2*, 180; (b) Macias, E.E.; Ratnasamy, P.; Carreon, M.A.; *Catalysis Today* **2012**, *198*, 215.
43. Srivastava, R.; Srinivas, D.; Ratnasamy, P.; *Appl. Catal. A.* **2005**, *289*, 128; (b) Srivastava, R.; Srinivas, D.; Ratnasamy, P.; *Catal. Lett.* **2003**, *89*, 81.
44. Wilson, S. T.; Broach, R.W.; Blackwell, C.S.; Bateman, C.A.; McGuire, N.K.; Kirchner, R.M.; *Microporous and Mesoporous Materials* **1999**, *28*, 125.

APPENDIX

Å	=	angstrom
a.u.	=	arbitrary unit
BET	=	Brunauer Emmett Teller
CO ₂	=	carbon dioxide
°C	=	Celsius
Cu	=	Copper
Pb	=	lead
θ	=	diffraction angle (degree)
SAPO	=	silicoaluminophosphate
<i>d</i>	=	d-spacing (Angstrom)
GC-MS	=	gas chromatograph – mass spectrometry
g	=	gram
mg	=	milligram
hr	=	hour
Kα	=	K-alpha x-rays
HT	=	hydrothermal
keV	=	kiloelectron volt
kV	=	kilovolt
ZIF	=	zeolite imidazole framework
psi	=	pounds per square inch
MW	=	microwave
Bio-MOF	=	metal-biomolecule framework
MOF	=	metal-organic framework
CH ₄	=	methane
ppm	=	parts per million
µm	=	micrometer
mm	=	millimeter
mA	=	milliamp
mL	=	milliliter
mmol	=	millimole
MHz	=	megahertz
MPa	=	Megapascal
min	=	minute
ms	=	millisecond
µs	=	microsecond
kPa	=	kilopascal
RPM	=	revolutions per minute

SEM	=	scanning electron microscopy
s	=	second
μ s	=	microsecond
NMR	=	nuclear magnetic resonance
EDS	=	energy-dispersive x-ray spectroscopy
SAED	=	selected area electron diffraction
TEM	=	transition electron microscopy
H ₂ O	=	water
TPD	=	temperature programmed desorption
XRD	=	x-ray diffractometry
MAS	=	magic angle-spinning

CURRICULUM VITAE

NAME: Zhenzhen Xie

ADDRESS: Department of Chemical Engineering
University of Louisville
Louisville, KY 40292

DOB: Hebei, China – September 12, 1988

EDUCATION & TRAINING:

B.S., Material Chemistry
Heilongjiang University
2007-2011

M.Eng., Chemical Engineering
University of Louisville
2011-2013

PUBLICATION:

Xie, Z., Zhu, M., Nambo, A., Jasinski, J.B., Carreon, M.A.,
“Microwave-assisted synthesized SAPO-56 as a catalyst in
the conversion of CO₂ to cyclic carbonates”, Dalton
Transactions, 2013, 42, 6732-6735,

PRESENTATION:

“Microwave-assisted synthesized SAPO-56 as a catalyst in
the conversion of CO₂ to cyclic carbonates” AICHE annual
meeting, Pittsburgh, October, 2012.